International Journal of Power and Energy Systems, Vol. 43, No. 10, 2023
An Open Access Paper

OPTIMAL REGULATION MODEL OF INTEGRATED ENERGY SYSTEM CONTAINING HYDROGEN STORAGE CONSIDERING ELECTROTHERMAL COUPLING

Xuan Wen*,**

Abstract

As an important way to improve energy efficiency, IES plays a key role in promoting sustainable development of energy. In order to optimise the regulation effect of hydrogen storage IES, from the perspective of electrothermal coupling, the optimisation regulation model of hydrogen storage IES was constructed, and its effectiveness was tested. The results show that under this control strategy, the consumption of wind power, photovoltaic power, and hydrogen power generation is maintained in the range of 2,500–3,500 kWh, 1,500–2,500 kWh, and 3,500–4,500 kWh, respectively. Compared with the control strategy without considering the electric heating coupling, the coal consumption per unit time under this method is reduced by 40–80 J. This shows that the regulation method has improved the consumption of clean energy, greatly reduced coal consumption and economic costs, improved the utilisation rate of clean energy, optimised the regulation effect of IES, and is conducive to promoting the development of renewable energy.

Key Words

Electrothermal, hydrogen energy storage, particle swarm algorithm, IES

1. Introduction

As a green energy source, hydrogen energy can replace fuel energy sources, such as natural gas and coal by using the chemical reaction of hydrogen to produce huge energy, and at the same time, hydrogen energy does not produce pollutants during the energy release process, which is more environmentally friendly compared to traditional energy sources [1], [2]. The application of hydrogen energy in the energy industry is embodied in the hydrogen energy storage system. By using hydrogen energy as a bridge to convert clean energy, such as light and heat energy to electricity, the hydrogen energy storage system can reduce unnecessary energy waste while improving the environmental protection of energy system operation [3]. In the hydrogen energy storage system, integrated energy system (IES) realises energy dispatching and utilisation through integration, planning, and collaborative management of multiple energy sources to meet diversified energy needs of various fields of society, avoid conflicts between different energy systems in operation, and improve the efficiency and coordination of energy use [4]. However, in the actual operation process, due to the difference of energy systems, the lack of attention to the degree of electrothermal coupling of power systems leads to the complementary utilisation between multiple energy sources is not fully utilised and the IES operation has little effect. For this reason, this study proposed the optimal regulation method of electrothermal-coupled hydrogen energy storage IES to promote the development of hydrogen energy storage technology and the construction of a new pattern of low-carbon development.

2. Related Work

Clean energy, including hydrogen energy, is an important way to control the total amount of carbon dioxide emissions and plays an important role in the process of carbon reduction. Carley and Konisky [5] aim to study the impact of clean energy transformation on equity and justice and take the northern part of the world as an example to analyse the differences in opportunities and interests arising from energy transformation, thus promoting the improvement of the quality of energy transformation. Hosseini and Wahid expounded the importance of hydrogen energy in the future

* Beijing Key Laboratory of Demand Side Multi-Energy Carriers Optimization and Interaction Technique, China Electric Power Research Institute, Beijing 100192, China; e-mail: 406100220010@email.ncu.edu.cn
** School of Information Engineering, Nanchang University, Nanchang 330031, China
Corresponding author: Xuan Wen
(DOI: 10.2316/J.2023.203-0500)

world and put forward the method of solar hydrogen production, so as to make the energy system integration more mature and promote the development of hydrogen energy utilisation [6]. In order to alleviate the harm of solid fuel combustion to the environment, Carter *et al.* studied the determinants and trends of solid fuel discontinuation in the household environment, so as to provide reference for the use of clean fuel in the household [7].

In addition, Su *et al.* analysed the importance of the stable security region of IES and introduced the process of its feature derivation. To improve the limitation of linear simplification under the traditional derivation method, a robust calculation method was proposed. In this way, the calculation error is reduced and the effectiveness of this method is proved [8]. Taking IES as the research object, Li *et al.* [9] proposed an IES reliability evaluation method combined with sequential Monte Carlo to effectively improve the safety and reliability of power supply system operation. In view of the poor cooperation between independent IES systems, Wang *et al.* designed a new energy trading model under the guidance of bargaining game theory. This will improve the sense of fairness of participants, reduce industrial costs, and increase individual interests [10].

From the above research results that with the development and progress of society, clean energy, such as hydrogen, has high application value in the industrial and domestic environment, and in energy utilisation, many scholars have put forward corresponding IES regulation schemes. However, from the perspective of electrothermal coupling, there are few studies on hydrogen-containing energy storage IES. To this end, the optimisation and control method of electrothermal coupling hydrogen energy storage IES is proposed to enrich the coordinated control theory of hydrogen energy storage IES and enhance the complementary use of various energy sources to achieve efficient, clean, and reliable energy supply.

3. Optimal Regulation Model of IES for Electrothermal Coupling Hydrogen Storage

3.1 Structure and Mathematical Model of Hydrogen-Containing IES

Electrothermal coupling improves the stability of the power system load and avoids unnecessary energy waste by peak shaving and valley filling. Electrothermal coupling is incorporated into hydrogen-containing IES with a view to improving the limitations of low coupling among energy sources in hydrogen storage systems and improving the reliability and stability of the energy supply. It also enhances the peaking capability of the energy system, thus realising the purpose of saving energy and protecting the environment [11]. In the wind power generation model, assuming that the external factors, such as air density and fan blade radius do not change, v_a and v_b denote the turbine cut-in speed and cut-out speed, respectively, the wind power output $P_{WT}(t)$ is calculated as shown in (1).

$$P_{WT}(t)=\begin{cases}0 & v(t)\geq v_b\\ P_R & v_r\leq v(t)<v_b\\ \frac{v(t)^3-v_a^3}{v_r^3-v_a^3} & v_a\leq v(t)<v_r\\ 0 & v(t)<v_a\end{cases} \tag{1}$$

In (1), P_R andv_r represent the rated power and wind speed of the turbine, respectively, and v_t represents the wind speed at t at the moment. In the PV power generation model, the light intensity at the moment of t is G, the ambient temperature is $T_d(t)$, the light intensity of the cell is $G_c(t)$ and its surface temperature is T, then its actual surface temperature $T_c(t)$ and output power $P_{pv}(t)$ are calculated in (2).

$$\begin{cases}T_c(t)=T_d(t)+\frac{G_c(t)}{800}\times(T-20)\\ P_{pv}(t)=P\frac{G_C(t)}{G}\left\{1+k_p[T_c(t)-T]\right\}\end{cases} \tag{2}$$

In (2), P and k_p are the maximum output power and power temperature factor of the battery, respectively. In the electric energy storage model, the battery is chosen as the electric energy storage device with an AC–DC conversion efficiency of β_{BAT}, its charging power and efficiency at $P_{BAT-ch}(t)$ and at the moment of $\beta_{BAT-ch}t$, and its discharging power and efficiency at $P_{BAT-dis}(t)$ and $\beta_{BAT-dis}$, respectively, and the actual capacity of the battery at this moment of $S(t)$ is calculated in (3).

$$S(t)=\frac{E_{BAT}(t-1)\times(1-\alpha)}{C_{BAT}}+\frac{\left[P_{BAT-ch}(t)\beta_{BAT}\beta_{BAT-ch}-\frac{P_{BAT-dis}(t)}{\beta_{BAT}\beta_{BAT-dis}}\right]}{C_{BAT}}\times 100\% \tag{3}$$

In (3), α, C_{BAT}, and E_{BAT} represent the charge retention capacity, rated capacity, and electrical energy storage capacity of the battery, respectively. In the hydrogen energy system model, hydrogen is mainly produced from the electrolyzer, m_{ET} denotes the hydrogen production rate of the electrolyzer equipment, P_{ET} denotes the electric power from the busbar, based on which the power flowing from the equipment to the hot busbar under electrothermal coupling is obtained at this moment $L_{EL}(t)$, which is calculated as shown in (4).

$$L_{EL}(t)=\delta(1-\delta_{EL})P_{EL}(t) \tag{4}$$

In (4), δ and δ_{EL} denote the heat transfer efficiency and hydrogen heat transfer efficiency, respectively. The generation power, converter efficiency, and working efficiency of the fuel cells are P_{FC}, γ_{FC-DC}, and γ_{FC}, respectively, then the expressions of hydrogen consumption rate m_{FC}, electrical power $P_{FC-BUS}(t)$, and heat transfer to the thermal bus $L_{FC}(t)$ of the cell are shown in (5).

$$\begin{cases}m_{FC}=P_{FC}(t)/\gamma_{FC}LHV_{H_2}\\ P_{FC-BUS}(t)=\gamma_{FC-DC}(1-\gamma_{FC})P_{FC}(t)\\ L_{FC}(t)=\gamma(1-\gamma_{FC})P_{FC}(t)/\gamma_{FC}\end{cases} \tag{5}$$

In (5), LHV_{H_2} represents the low heating value of hydrogen and γ represents the heat transfer efficiency of the cell. The calculation of the energy stored in the hydrogen tank $E(t)$ at that moment is shown in (6).

$$E(t) = E(t-1) + \left[\delta_{EL} \times \delta_{EL-DC} \times P_{EL}(t-1) - \frac{P_{FC}(t-1)}{\gamma_{TANK} \times \gamma_{FC} \times \gamma_{FC-DC}}\right] \times \triangle t \tag{6}$$

In (6), γ_{TANK}, $\triangle t$, and δ_{EL-DC} represent the storage tank efficiency, time difference, and electrolyzer converter efficiency, respectively. Hydrogen is produced using an electrolyzer and fed into a hydrogen storage tank for storage, while a fuel cell obtains hydrogen from it for power generation according to actual needs. $P^{th}_{CHP,\max}$ denotes the maximum heating power of the unit, P^{e}_{CHP} denotes the power generated by the pure condensing unit, l_1 and l_2 denote the difference of the unit output when the inlet gas is the maximum and the minimum, respectively, and l_3 denotes the backpressure elastic operating coefficient, then the expression of the CHP model is shown in (7).

$$\begin{cases} \max\left\{ \begin{array}{l} P^{e}_{CHP,\min} - l_2 \cdot P^{th}_{CHP,t} \\ l_3 \cdot (P^{th}_{CHP,t} - P^{th}_{CHP,t_0}) \end{array} \right\} \le P^{e}_{CHP} \\ P^{e}_{CHP} \le P^{e}_{CHP,\max} - l_1 \cdot P^{th}_{CHP,t} \\ 0 \le P^{th}_{CHP,t} \le \cdot P^{th}_{CHP,\max} \end{cases} \tag{7}$$

In (7), $P^{e}_{CHP,\min}$ and $P^{e}_{CHP,\max}$ denote the minimum and maximum power generation of the unit in the pure condensing state, respectively, and P^{th}_{CHP,t_0} and $P^{th}_{CHP,t}$ denote the heat supply power at the initial state and t, respectively. The thermal storage tank is the main equipment for thermal energy storage, and its thermal storage state and thermal energy storage at t are $H(t)$ and $HOC(t)$, respectively, and its converter efficiency is ρ, then the thermal energy storage system model is expressed as shown in (8).

$$\begin{cases} HOC(t) = \frac{H(t)}{C} \times 100\% \\ H(t) = H(t-1) + \left[H(t)'\rho\rho' - \frac{H(t)^{\&}}{\rho\rho^{\#}}\right] \triangle t \end{cases} \tag{8}$$

In (8), C denotes the rated capacity of the thermal storage tank, $H(t)'$ and ρ' denote the thermal storage power and efficiency, respectively, and $H(t)^{\&}$ and $\rho^{\#}$ denote the exothermic power and efficiency, respectively. The structure of the hydrogen-containing IES considering electrothermal coupling is shown in Fig. 1.

In Fig. 1, the electric energy system model, the hydrogen energy system model, and the thermal energy system model together form an electrothermal-coupled hydrogen-containing IES. Each system model mainly consists of an energy preparation model and a storage model to complete the production and output of energy and flexibly meet the actual energy demand.

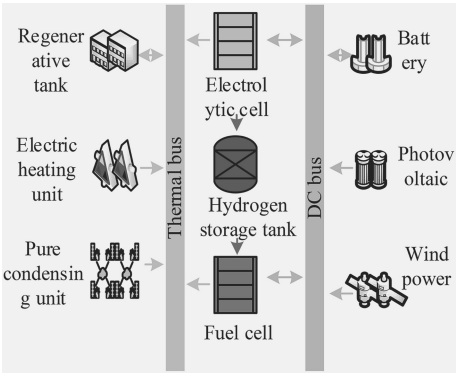

Figure 1. Hydrogen-containing IES structure considering electrothermal coupling.

3.2 Multi-energy Coupling Model Analysis

In the context of ecological civilisation construction, promoting energy transformation and building a clean and low-carbon energy system has become an important part of the energy production and consumption revolution, At the same time, through the regulation of each energy source, the barriers between energy systems can be broken, the transposition and deployment of energy sources can be realised, and the coordination and optimisation between multiple energy sources can be promoted. In the IES containing hydrogen storage, the main source of coal consumption is in the thermal energy system, so the objective function of IES regulation should be set according to the three operation modes of pumped cogeneration units, backpressure cogeneration units, and pure condensing units. For the pumped cogeneration unit constraint, the thermal power constraint is expressed as shown in (9).

$$0 \le P^{th}_{CHP,j,h} \le P^{th}_{CHP,j,\max} \tag{9}$$

In (9), $P^{th}_{CHP,j,\max}$ indicates the maximum thermal power output of the unit j, and $P^{th}_{CHP,j,h}$ indicates the thermal power of the unit at the moment t. The expression of the electric power constraint of the pumped cogeneration unit is shown in (10).

$$\begin{cases} P^{e,t}_{CHP,j} \ge \max\left\{ \begin{array}{l} P^{e}_{CHP,j,\min} - l_{2,j} \cdot P^{th,t}_{CHP,j.h}, l_{3.j} \\ \cdot (P^{th.j}_{CHP,j,h} - P^{th}_{CHP,j,h_0}) \end{array} \right\} \\ P^{e,t}_{CHP,j} \le P^{e}_{CHP,j,\max} - l_{1,j} \cdot P^{th,t}_{CHP,j,h} \end{cases} \tag{10}$$

In (11), $l_{1,j}$ and $l_{2,j}$ indicate the difference of the output power of the unit j when the inlet air volume is maximum and minimum, respectively, and $l_{3,j}$ indicates the backpressure elastic operating factor of the unit. j, $P^{e}_{CHP,j,\max}$ and $P^{e}_{CHP,j,\min}$ indicate the maximum and minimum electrical power of the unit when pumping, respectively, and P^{th}_{CHP,j,h_0} indicates the corresponding constant value of the unit. As the backpressure and pure condensing units have the same heating source, the constraints are the same for both. For the constraint of the electrical energy system, the number of heating zones is N, and the sum of pumped and backpressure units in the

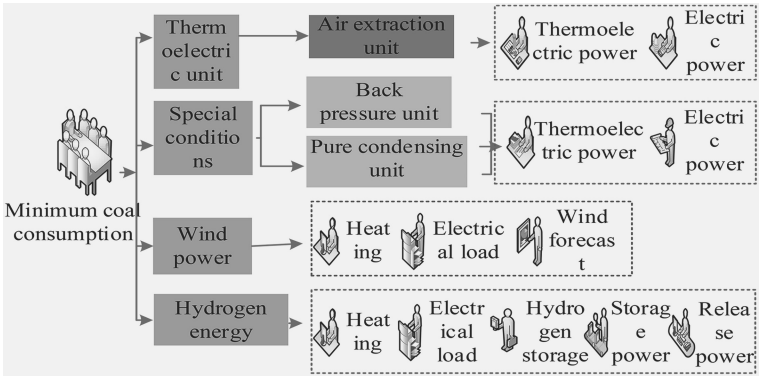

Figure 2. Structure of multi-energy coupling model with the goal of minimising total coal consumption.

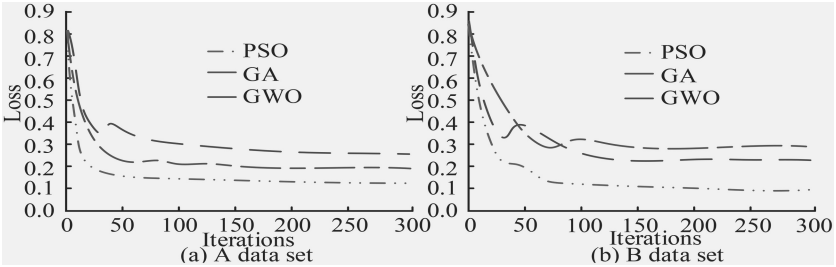

Figure 3. Comparison of loss values of different algorithms.

heating zone numbered is r, G_{CHP}^{r}, and G_{b}^{r}, respectively; the wind power feed-in at the moment t is P_{w}^{t}, then the constraints on the heating, electrical load, and wind power forecasts are shown in (11).

$$\begin{cases} \sum_{j\in G_{b}^{r}\cup G_{CHP}^{r}} P_{j}^{th,t} \geq H_{D,r}^{t} \\ \sum_{j\in O} P_{j}^{e,t} + P_{w}^{t} - P_{ex}^{t} = P_{EL}^{e,t} \\ P_{ex,\min} \leq P_{ex}^{t} \leq P_{ex,\max} \\ P_{w}^{t} \leq P_{w,p}^{t} \end{cases} \tag{11}$$

In (11), $H_{D,r}^{t}$ represents the thermal energy demand in the region of r, O represents the sum of units, $P_{j}^{e,t}$ and P_{ex}^{t} represent the generation power of unit j and the exchange rate of the electric energy system at the moment of t, respectively, $P_{EL}^{e,t}$ and $P_{w,p}^{t}$ represent the predicted values of electric load and wind power, respectively, and $P_{ex,\min}$ and $P_{ex,\max}$ represent the minimum and maximum values of the exchange power of the electric energy system, respectively. For the constraint of the hydrogen energy system, the hydrogen energy stored in the r region after the hydrogen production at the time of t is $\triangle S_{H_2,r}^{t}$, and the total amount of hydrogen energy stored at this time is $S_{H_2,r}^{t}$, then the constraint expression for the heat supply, electric load, and hydrogen storage of the hydrogen energy system is shown in (12).

$$\begin{cases} \sum_{j\in G_{b}^{r}\cup G_{CHP}^{r}} P_{j}^{th,t} + P_{H_2,r}^{th,t} \geq H_{D,r}^{t} \\ \sum_{j\in O} P_{j}^{e,t} + P_{w}^{t} - P_{ex}^{t} = P_{EL}^{e,t} + \triangle S_{H_2,r}^{t} \\ S_{H_2,r}^{t} = S_{H_2,r}^{t-1} + \triangle S_{H_2,r}^{t} - P_{H_2,r}^{th,t} \end{cases} \tag{12}$$

In (12), $P_{H_2,r}^{th,t}$ represents the heat output power used for compensation at t in the r region at the moment. The maximum hydrogen discharge and storage power for hydrogen energy storage are $P_{H_2,r,\max}^{th}$ and $\triangle S_{H_2,r,\max}$, respectively, and the constraints on the hydrogen storage and discharge rates of the hydrogen energy storage system are given in (13).

$$\begin{cases} \triangle S_{H_2,r}^{t} \leq S_{H_2,r,\max} \\ P_{H_2,r}^{th,t} \leq P_{H_2,r,\max}^{th,t} \end{cases} \tag{13}$$

In (13), $S_{H_2,r,\max}$ denotes the maximum capacity of hydrogen energy storage. The structure of the coupled multi-energy model with the objective of minimising the total coal consumption is shown in Fig. 3.

In Fig. 2, the objective of the multi-energy coupling model is to minimise coal consumption and to constrain the systems, such as electrical energy and hydrogen energy, and to limit the output and output of electrical and thermal energy of the cogeneration unit due to the electric and thermal coupling characteristics.

3.3 PSO-based IES Optimal Regulation Model Solving

Particle swarm optimisation (PSO) is a biological heuristic method that originated from the study of bird foraging behaviour. The core idea of PSO is to achieve information sharing among groups through coordination and cooperation among individuals, and to complete the search for optimal solutions on this basis. In the IES optimal regulation model solution, the particle population

size is set as M, the spatial dimension is D, the individual optimal solution of the particle is P_{best}, the optimal solution of the particle swarm is G_{best}, the first i particle is i, the dimensions of each particle include $u(i)$, $w(i)$, and $q(i)$, which denote the heat output, electricity output, and wind power feed-in capacity of the thermoelectric unit, respectively, and the velocity and position of each particle in the three dimensions are initialised, where the velocity is expressed as shown in (14).

$$\begin{cases} v_{u(i)} = \alpha * [v_{u(i),\max} - v_{u(i)}] + v_{u(i)} \\ v_{w(i)} = \alpha * [v_{w(i),\max} - v_{w(i)}] + v_{w(i)} \\ v_{q(i)} = \alpha * [v_{q(i),\max} - v_{q(i)}] + v_{q(i)} \end{cases} \tag{14}$$

In (14), $v_{u(i)}$, $v_{w(i)}$, and $v_{q(i)}$ denote the velocities of the particles in the thermal output, electrical output, and wind power feed-in capacity dimensions, respectively, $v_{u(i),\max}$, $v_{w(i),\max}$, and $v_{q(i),\max}$ denote the velocity maxima in the three dimensions, and α denotes a random number uniformly distributed in the range [0, 1]. The expressions for the positions of the particles in the three dimensions are given in (15).

$$\begin{cases} x_{u(i)} = \alpha * [x_{u(i),\max} - x_{u(i),\min}] + x_{u(i),\max} \\ x_{w(i)} = \alpha * [x_{w(i),\max} - x_{w(i),\min}] + x_{w(i),\max} \\ x_{q(i)} = \alpha * [x_{q(i),\max} - x_{q(i),\min}] + x_{q(i),\max} \end{cases} \tag{15}$$

In (15), $x_{u(i)}$, $x_{w(i)}$, and $x_{q(i)}$ denote the positions of the particles in the thermal, electrical, and wind power online capacity dimensions, $x_{u(i),\min}$, $x_{w(i),\min}$, and $v_{q(i),\min}$ denote the minimum values of the particles in the three dimensions, and $x_{u(i),\max}$, $x_{w(i),\max}$, and $v_{q(i),\max}$ denote the maximum values of the particles in the three dimensions. The velocity and position range of the particle search, to provide direction for the search and avoid blind search, then the particle search range is expressed in (16).

$$\begin{cases} X_{\min} \le x(i) \le X_{\max} \\ V_{\min} \le v(i) \le V_{\max} \end{cases} \tag{16}$$

In (16), $x(i)$ and $v(i)$ denote the position and velocity of the particle, respectively, $X_{\max}$ and $X_{\min}$ denote the maximum and minimum value of the position, respectively, and $V_{\max}$ and $V_{\min}$ denote the maximum and minimum value of the velocity, respectively. To improve the efficiency and quality of particle search, an adaptation function is needed to evaluate the degree of merit of each particle. At the same time, to balance the global and local search ability of the particle, it is necessary to use the inertia weight. Through iterations, the particle fitness values are calculated and updated based on P_{best} and G_{best} until the maximum number of iterations is reached and the optimal values of thermal output, electric output, and wind power feed-in capacity are output.

4. Application of Electrothermal Coupling for Optimal Regulation Model of Hydrogen-containing IES

4.1 Algorithm Performance Analysis

Datasets A and B are selected for algorithm performance testing, where Dataset A is from the Elia dataset and Dataset B is from the DR Power dataset. In both datasets A and B, 75% of them are randomly selected as the training set, 15% as the test set, and 10% as the validation set. The loss value and F1 value are used as algorithm performance evaluation indexes, and genetic algorithm (GA) and grey wolf optimiser (GWO) are also added as experimental comparisons. The comparison of loss values of different algorithms is shown in Fig. 3.

In Fig. 3, in the test and training of dataset A, PSO tends to be stable after 50 iterations, and the loss value reaches 0.15; GA reaches 0.2 loss value after 100 iterations; GWO has the highest loss value of 0.3 at about 50 iterations. In the test and training of dataset B, the PSO loss value is the lowest of all algorithms, 0.1; Compared with PSO, GA, and GWO loss values increased by 0.15 and 0.2, respectively. Thus, PSO accelerates the convergence speed and reduces the loss value of model solution. A comparison of F1 values for different algorithms is shown in Fig. 4.

In Fig. 4, the F1 value of PSO in dataset B remains within the range of 0.85–0.92, which is about 0.5 higher than the F1 value in dataset A; the F1 value of GA in dataset B is 0.73 at the lowest and 0.83 at the highest; the F1 value of GWO can reach 0.85 at most, and the global optimisation ability is poor. It can be seen that the F1 value of PSO is the highest in the training and testing process, which means that its optimal solution search effect is the best, which is conducive to laying a good foundation for IES regulation.

4.2 Analysis of Optimal Regulation Results

To reflect the effect of optimal regulation, a typical winter day is selected for the experiment, with a 24-h dispatch period and a minimum dispatch time of 1 h. The energy output, clean energy consumption, and coal consumption per unit time are collected and analysed throughout the day. In the experimental process, the regulation method adopted in the study is recorded as strategy 1, and the regulation scheme of IES with hydrogen storage without electrothermal coupling is added as the experimental comparison and recorded as strategy 2. The wind power output, electrical load, thermal load, and hydrogen load of this hydrogen storage IES are predicted in Fig. 5.

In Fig. 5, the wind power output forecast of the system is kept in the range of 1,700–2,800 kW, the power load forecast is kept in the range of 900–1,800 kW, the heat load forecast value is concentrated in the range of 600–1,000 kW, and the hydrogen load forecast value reaches the maximum at 18:00, which is 1,400 kW. It can be seen that the change trend of wind power forecast and power

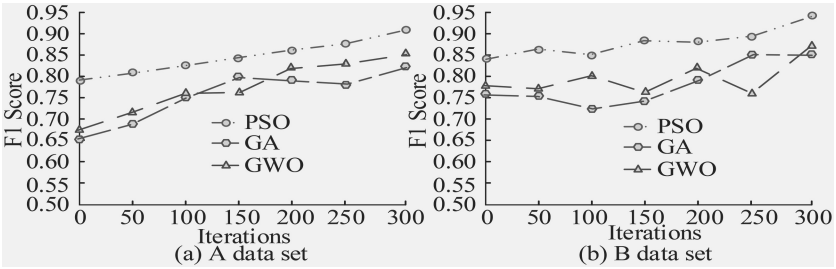

Figure 4. Comparison of F1 scores of different algorithms.

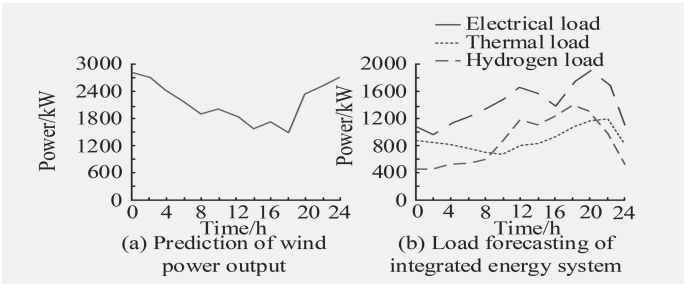

Figure 5. Basic data of integrated hydrogen storage energy system.

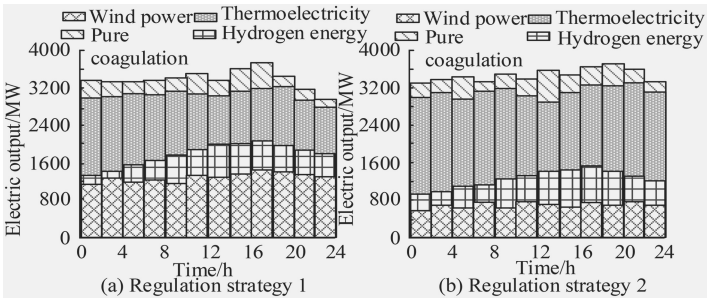

Figure 6. Comparison of energy output under different control strategies.

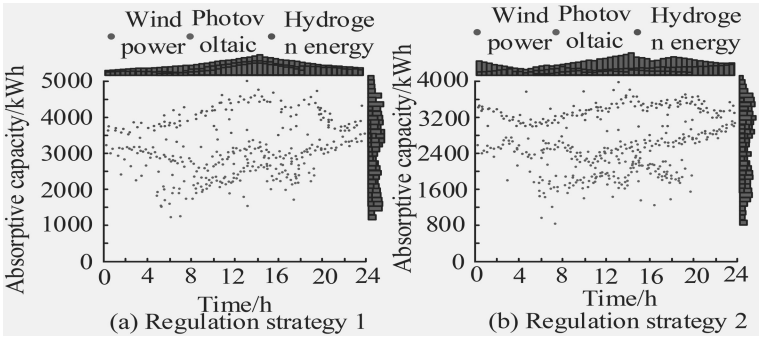

Figure 7. Comparison of clean energy consumption under different control strategies.

load forecast is basically opposite, which is caused by the reverse peak regulation characteristics of wind power. The comparison of energy output under different regulation strategies is shown in Fig. 6.

In Fig. 6, under the control of Strategy 1, the wind power output is concentrated at 1,200 MW; the output of thermal power unit is kept within the range of 1,200–3,000 MW; the hydrogen energy output is higher at 8–18 points, with a maximum of 2,000 MW; the maximum value of pure condensing output is 2,800 MW. In the regulation of Strategy 2, thermal power units and pure condensing units are mainly responsible for the output of IES, and the output of wind power and hydrogen energy is significantly reduced. It can be seen that Strategy 2 enhances the coupling between various energies and significantly improves the utilisation rate of clean energy. The comparison of clean energy consumption under different regulation strategies is shown in Fig. 7.

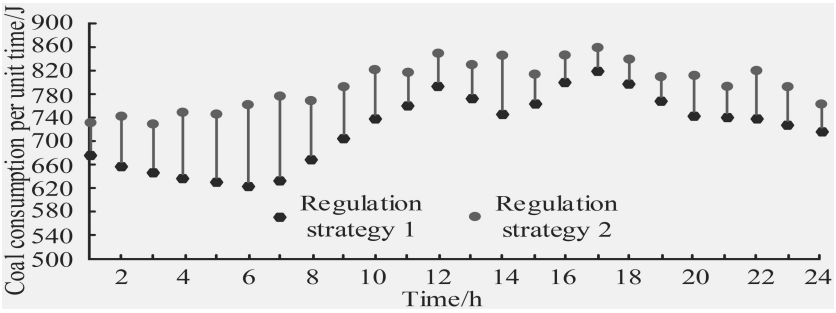

Figure 8. Comparison of coal consumption per unit time under different control strategies.

From Fig. 7, under the control of Strategy 1, the wind power generation capacity changes in the range of 2,500–3,500 kWh, which is 300–500 kWh higher than that of Strategy 2; the consumption of photovoltaic power generation shall be kept within the range of 1,500–2,500 kWh; the consumption of hydrogen power generation reaches the maximum at 14:00, 4,500 kWh. Compared with the maximum value of hydrogen power generation consumption in Strategy 2, it is increased by 900 kWh. This shows that Strategy 2 reduces the waste of new energy and greatly improves the consumption level of clean energy. The comparison of coal consumption per unit time under different control strategies is shown in Fig. 8.

In Fig. 8, under the control of Strategy 1, the coal consumption per unit time changes in the range of 620–780 J, with the highest coal consumption per unit time at 17:00; under the control of Strategy 2, the coal consumption per unit time is concentrated in the range of 740–820 J, which is about 40–80 J higher than that of Strategy 1. The reason is that Strategy 2 has improved the utilisation rate of wind power at night, and the proportion of thermoelectric units has decreased. It can be seen that Strategy 2 significantly reduces the amount of coal used per unit time is conducive to environmental protection and improves the effect of IES optimisation and control.

5. Conclusion

To improve the regulation effect of hydrogen storage IES, the optimisation regulation method of hydrogen storage IES based on electrothermal coupling is proposed, and its application effect is tested and analysed. In the test and training of the algorithm, the minimum number of iterations of PSO is 50, the minimum loss value is 0.1, and the maximum F1 value can reach 0.92, which is 0.1 and 0.13 higher than GA and GWO, respectively. Under the control strategy studied, wind power output is concentrated at 1,200 MW, and hydrogen energy output can reach 2,000 MW at most; the consumption of wind power generation varies in the range of 2,500–3,500 kWh, and the consumption of photovoltaic power generation remains in the range of 1,500–2,500 kWh; the coal consumption per unit time varies in the range of 620–780 J, which is about 40–80 J lower than that of strategy 2. In general, this optimised regulation method improves the flexibility of IES energy regulation, enhances the coupling between multiple types of energy, and reduces the economic cost of IES operation, which can provide assistance for promoting the comprehensive green transformation of economic and social development. However, there are still limitations of insufficient experimental samples. In future research, it is necessary to expand the experimental samples.

Funding Statement

The work was financially supported by 2022 Open Fund Project of Beijing Key Laboratory of Demand Side Multi-Energy Carriers Optimization and Interaction Technique, (Research on Optimal Operation of Integrated Energy Systems with Hydrogen Storage System Considering Source-load Uncertainty, YDB51202201360).

References

[1] J. Zhang, H. Cho, P.J. Mago, H. Zhang, and F. Yang, Multi-objective particle swarm optimization (MOPSO) for a distributed energy system integrated with energy storage, *Journal of Thermal Science*, *28*(2), 2019, 1221–1235.

[2] F. Shahzad, J. Bouslimi, S. Gouadria, J. Wasim, R.E. Mohamed, S. Rabia, S. Md, and S.N. Kottakkaran, Hydrogen energy storage optimization in solar-HVAC using Sutterby nanofluid via Koo-Kleinstreuer and Li (KKL) correlations model: A solar thermal application, *International Journal of Hydrogen Energy*, *47*(43), 2022, 18877–18891.

[3] P. Liu, T. Ding, Z. Zou, and Y. Yang, Integrated demand response for a load serving entity in multi-energy market considering network constraints, *Applied Energy*, 250(PT.1), 2019, 512–529.

[4] M. Andrijevic, C.F. Schleussner, M.J. Gidden, and D.L. Mccollum, COVID-19 recovery funds dwarf clean energy investment needs, *Science*, *370*(6514), 2020, 298–300.

[5] S. Carley and D.M. Konisky, The justice and equity implications of the clean energy transition, *Nature Energy*, *5*(8), 2020, 569–577.

[6] S.E. Hosseini and M.A. Wahid, Hydrogen from solar energy, a clean energy carrier from a sustainable source of energy, *International Journal of Energy Research*, *44*(6), 2020, 4110–4131.

[7] E. Carter, L. Yan, Y. Fu, B. Robinson, F. Kelly, P. Elliott, Y. Wu, L. Zhao, M. Ezzati, X. Yang, Q. Chan, and J. Baumgartner, Household transitions to clean energy in a multiprovincial cohort study in China, *Nature Sustainability*, *3*(1), 2020, 42–50.

[8] J. Su, H.D. Chiang, Y. Zeng, and N. Zhou, Toward complete characterization of the steady-state security region for the electricity–gas integrated energy system, *IEEE Transactions on Smart Grid*, *12*(4), 2021, 3004–3015.

[9] Z. Li, Z. Wang, Y. Fu, and N. Zhao, Energy supply reliability assessment of the integrated energy system considering complementary and optimal operation during failure, *IET Generation Transmission & Distribution*, *15*(13), 2021, 1897–1907.

[10] Y. Wang, X. Wang, C. Shao, and N. Gong, Distributed energy trading for an integrated energy system and electric vehicle charging stations: A Nash bargaining game approach, *Renewable Energy*, *155*, Aug. 2020, 513–530.

[11] S. Lu, W. Gu, K. Meng, and Z. Dong, Economic dispatch of integrated energy systems with robust thermal comfort management, *IEEE Transactions on Sustainable Energy*, *12*(1), 2020, 222–233.

Biographies

Xuan Wen received the B.S. degree in interior design from GUET in 2020. He is currently pursuing the master's degree with the School of Information Engineering, NCU. His fields of interest include integrated energy system optimisation and demand-side management.